Том 34, Номер 6

Ноябрь - Декабрь 1996

ISSN 0023-4206

РОССИЙСКАЯ АКАДЕМИЯ НАУК

КОСМИЧЕСКИЕ ИССЛЕДОВАНИЯ

Главный редактор
Л.И. Седов

МАИК "НАУКА" "НАУКА"

Cosmic Research, Vol. 34, No. 6, 1996, pp. 559–566. Translated from Kosmicheskie Issledovaniya, Vol. 34, No. 6, 1996, pp. 604–612.

Solar Wind Deceleration Upstream of the Martian Bow Shock: Possible Influence of Dense Corona of Neutral Gas

G. Kotova*, M. Verigin*, A. Remizov*, H. Rosenbauer, K. Szegö***, J. Slavin****, M. Tatrallyay***, K. Schwingenschuh*****, and N. Shutte***

**Space Research Institute, Russian Academy of Sciences, ul. Profsoyuznaya 84/32, Moscow, 117810 Russia*
***Max-Planck-Institut für Aeronomie, Katlenburg-Lindau, Germany*
****Central Research Institute for Physics, Budapest, Hungary*
*****NASA Goddard Space Flight Centre, Greenbelt, Maryland, USA*
******Institut für Weltraumforschung, Graz, Austria*

Received December 5, 1995

Abstract—A deceleration of the solar wind upstream of the Martian bow shock near the terminator plane is analyzed using data of the TAUS spectrometer on board the *Phobos 2* spacecraft. The value of the velocity decrease upstream of the Martian bow shock for outbound orbit parts (on average these cases correspond to crossings of the quasi-parallel shock wave) is inversely proportional to the density of the undisturbed solar wind, but practically there is no such dependence for inbound orbit segments, which are, on average, attributed to crossings of the quasi-perpendicular shock wave. This fact can be explained by the existence of an extended corona of neutral particles near Mars that causes the solar wind deceleration upstream of the shock wave; however, in the case of crossing quasi-perpendicular shock wave, an important role is played by the strong mass loading of the solar wind by reflected protons. The obtained dependence of the velocity decrease upstream of the bow shock on the density of the undisturbed solar wind allows one to estimate the density of neutral particles in the Martian corona.

INTRODUCTION

Verigin *et al.* [1] considered a deceleration of the solar wind upstream of the Martian bow shock using data of the TAUS experiment on board the *Phobos 2* spacecraft in its first three elliptical orbits near Mars. The velocity decrease of the solar wind upstream of the bow shock near the subsolar point was about 100 km/s. It should be stressed that the deceleration can be caused by the mass loading of plasma flow by ions originating from the oxygen/hydrogen corona of Mars and/or by protons reflected from the bow shock. The limiting hot oxygen density profile in the corona and the upper limit of the rate of oxygen loss by the planet were estimated, taking into account only the influence of the Martian oxygen corona. However, the estimates of the oxygen corona density obtained were 5 times higher than the maximum theoretical value calculated by the model of Ip [2, 3].

Barabash and Lundin [4] studied the deceleration of the solar wind upstream of the bow shock in the third elliptical orbit using the data of the ASPERA experiment. It follows from their estimates that about 60% of the observed solar wind deceleration was connected with protons specularly reflected from the bow shock. Dubinin *et al.* [5], analyzing the data of the ASPERA experiment obtained in first four *Phobos-2* orbits, revealed an asymmetry of the plasma density increase in front of the bow shock. They attributed this asymmetry to a change in the interplanetary magnetic field orientation.

According to theoretical [6–8] and experimental [9, 10] investigations of the Earth's bow shock, the density of reflected protons may be up to 20–30% of the incoming density of the solar wind in the case of a quasi-perpendicular wave. These ions are later turned by the solar wind magnetic field and quickly come back to the bow shock. The solar wind deceleration occurs at small distances from the bow shock $\leq r_{g\perp} = V_\perp/\omega_{gi}$, where $V_\perp$ is the solar wind velocity component perpendicular to the shock wave front, and ω_{gi} is the gyrofrequency of protons [9, 11]. The motion of the leading centre of specularly reflected protons is directed from the bow shock; however, their density is only ~3% of the incoming flow density of the solar wind [12] in the case of a quasi-parallel wave.

The solar wind deceleration, 7–10 km/s on average, is observed near the Earth in front of the quasi-parallel wave in the foreshock region [13, 14]. "Diffusive" ions flowing from the bow shock cause it. These ions should also exist near Mars in front of the quasi-parallel shock wave and should decelerate the flow of the solar wind.

In this work, we will attempt to consider different causes of solar wind deceleration in front of the bow shock based on the difference between ion reflection from quasi-perpendicular and quasi-parallel shock waves. The mass loading of the solar wind by ions

0010-9525/96/3406-0559$15.00 © 1996 МАИК Наука/Interperiodica Publishing

from the neutral corona of Mars implies that deceleration should be inversely proportional to the solar wind concentration. An analysis of this dependence will allow us to estimate the contribution of the Martian corona to the solar wind deceleration in front of the bow shock near the planet.

INSTRUMENTATION AND RAW DATA

This work is based on data of the TAUS and MAGMA experiments on board the *Phobos-2* spacecraft. The TAUS energy spectrometer was specially designed for studies of the solar wind and its interaction with Mars [15]. It allowed us to measure separately the spectra of protons, alpha-particles and heavy ions ($M/q > 3$, where M is the ion mass number and q is its charge) within the energy range per unit charge of ~30–6000 V, subdivided into 32 channels. The TAUS spectrometer had a field of view of ~40° × 40°, centered so as to adjust for solar wind aberration (~5° off the solar direction in the ecliptic plane), which was divided into 8 × 8 angular bins. Total proton spectrum was measured for 8 s. The MAGMA flux gate magnetometer had a range of ±100 nT resolution 0.05 nT and returned data at a rate of one vector in every 1.5 or 45 s depending on the telemetry mode [16].

The *Phobos-2* spacecraft was in a near circular orbit (~9500 km from the planet's center), quasi-synchronous with the orbit of the moon Phobos from February 20 to March 26, 1989. During this time interval, TAUS provided one proton spectrum in an energy range of 150–6000 eV every 2 min, and MAGMA measured one magnetic field vector every 45 s. Unfortunately, most of the time the *Phobos-2* spacecraft was rotating, and the angle between the axis of rotation and the Sun–Mars line sometimes was as large as ~20°. Thus, only the magnitude of the magnetic field vector will be used in this work.

The bow shock crossings were identified by a sudden decrease of the mean energy with simultaneous broadening in the proton spectra, and correlated increase of the magnetic field value [17, 18]. Data obtained just before the outermost crossings were considered in a case of multiple crossings of the bow shock.

EXPERIMENTAL RESULTS

Altogether, 41 inbound and 29 outbound magnetosphere crossings of the bow shock by the spacecraft were considered in analyzing the solar wind deceleration upstream of the Martian bow shock by data of the TAUS experiment. Simultaneous data of the magnetic field are available for 36 and 26 bow shock crossings, respectively. We excluded several crossings from our analysis because large variations of solar wind speed had been observed near the Martian bow shock.

The average angle between the spiral Martian magnetic field and the Sun–Mars line is ~56° near the orbit of Mars. Therefore, a quasi-perpendicular shock wave is observed more frequently on average on the dusk side for spacecraft entering into the planet's magnetosphere, and a quasi-parallel shock wave corresponds to the dawn side for spacecraft exiting from the magnetosphere. It is impossible to reliably determine the type of the shock wave, quasi-parallel or quasi-perpendicular, crossed by the spacecraft for any given case because of its rotation in most orbits. Some conclusions can be made only analyzing variations of the magnetic field magnitude during shock wave crossings.

Figure 1 presents examples of solar wind parameter variations for bow shock crossings during inbound and outbound passes of the magnetosphere. The spacecraft was rotating during both passes, but large regular variations of solar wind density were not observed, so the rotation axis (and, therefore the TAUS field of view) was pointed to the near Sun direction. A profile of the magnetic field variation with a distinctive shock foot and an overshoot shows that *Phobos-2* crossed the quasi-perpendicular shock wave at 23:37 UT on March, 2. The angle between the magnetic field direction and the shock wave normal was estimated using a model of the Martian bow shock [19, 20] and magnetic field data corrected for the rotation of the spacecraft (θ_{BN} ~67°). The spacecraft crossed the quasi-parallel shock wave at 03:19 UT on March 2 (θ_{BN} ~ 40°). It can be seen that a rather strong deceleration of the solar wind upstream of the bow shock is observed for the entry of the spacecraft into the magnetosphere, but a gradual deceleration of the solar wind is observed for the exit from the magnetosphere.

Figure 2 shows variations of average normalized parameters of solar wind protons upstream of the bow shock, their velocity V_{sw}, density N_{sw}, and temperature T_{sw}. It illustrates the difference between magnetopause crossings for outbound and inbound segments of the spacecraft orbit that reflects a difference between crossings of quasi-parallel and quasi-perpendicular shock waves. These parameters were averaged for a 20 min time interval centered by ~50 min apart from the bow shock crossing by the spacecraft. Figure 2a shows these parameters averaged for all bow shock crossings. The empty and solid circles correspond to inbound and outbound passes, respectively. The average deceleration of the solar wind upstream of the bow shock is ~7% of the solar wind velocity for inbound passes to the magnetosphere and ~4% for outbound passes. In addition, the deceleration is sharper in the former case. Such a strong deceleration for outbound orbit section is apparently caused by a large number of protons reflected from the quasi-perpendicular shock wave and concentrated near its foot. However, a more gradual deceleration of the solar wind approaching the bow shock for an inbound orbit section may be attributed to the mass loading of the flow by oxygen and hydrogen ions originating from the corona of

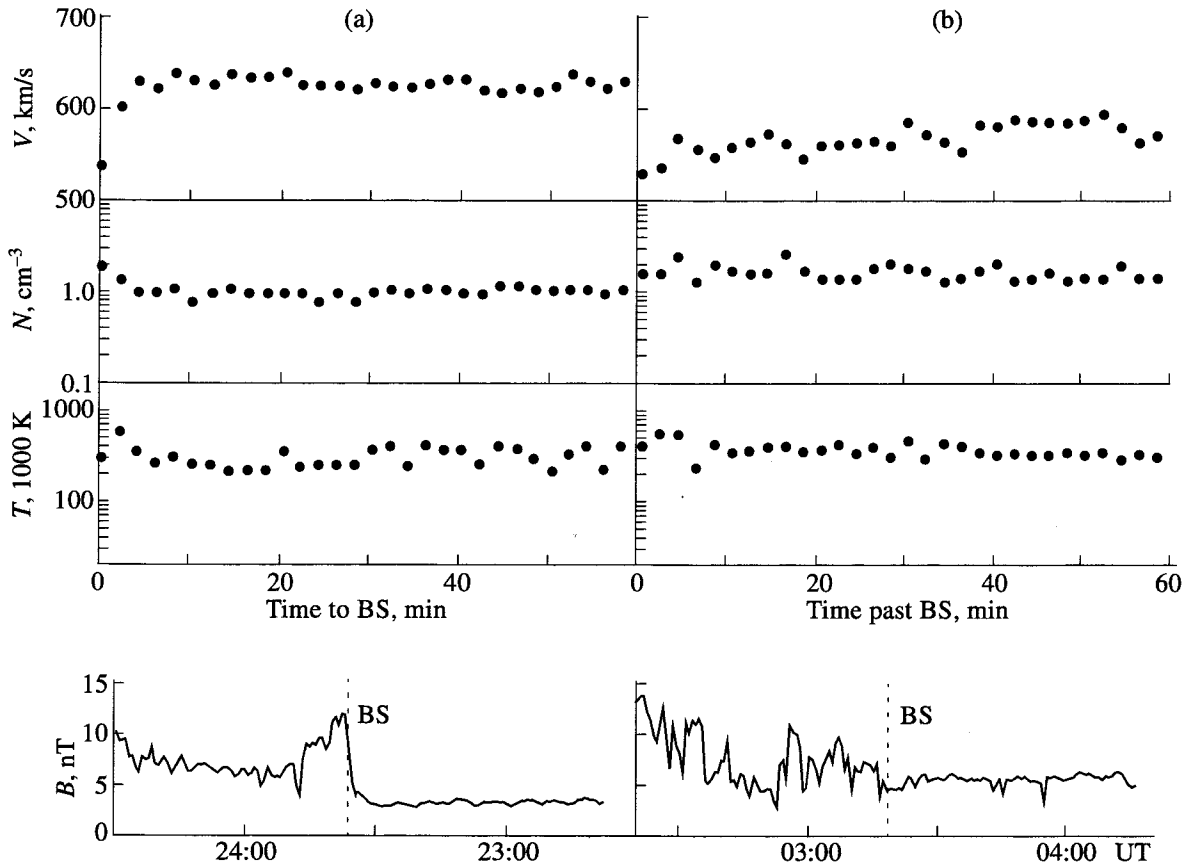

Fig. 1. Variations of parameters of the solar wind upstream of the bow shock (BS) near Mars for the satellite entry to the magnetosphere and exit out of it on March 2 at (a) 23:37 UT and (b) 03:19 UT, respectively.

Mars. The effect of coronal ions on the inbound pass through the magnetosphere is accompanied by a stronger mass loading of the flow by specularly reflected protons.

Figure 2b presents profiles of the normalized solar wind velocity, density, and temperature, which have been averaged depending on the ratio B_m/B_{sw}, where B_{sw} is the solar wind magnetic field averaged for the same time intervals as all other parameters, and B_m is the magnetic field in the transition region (magnetosheath) behind the overshoot. The empty and solid circles show average solar wind parameters corresponding to those shock wave crossings where the ratio B_m/B_{sw} was greater or less than 2.3, respectively. This separation of the data may reflect a difference between crossings of quasi-perpendicular and quasi-parallel shock waves (see Figs. 9 and 10 in [21], taking into account that the magnetosonic Mach number was greater than 3 for almost the entire time of circular *Phobos-2* orbits).The change of normalized parameters in Fig. 2b is similar to that in Fig. 2a. The difference between density profiles in Figs. 2a and 2b qualitatively corresponds to the asymmetry of density changes in front of the bow shock in the subsolar region discussed in [5].

Let us consider the dependence of solar wind deceleration on its density to check the relationship between the solar wind deceleration upstream of the bow shock and the mass loading of the flow by ions of planetary origin.

Verigin *et al.* [1] used the equations of hydrodynamic flow [22] accounting for the mass loading of the solar wind by ions of planetary origin:

$$\begin{aligned} \mathrm{div}(N\mathbf{V}) &= 0, \\ \mathrm{div}(\rho\mathbf{V}) &= Q, \\ \rho(\mathbf{V}, \nabla)\mathbf{V} &= -\nabla p - Q\mathbf{V}, \\ \mathrm{div}(\mathbf{V}(\rho V^2/2 + \gamma p/(\gamma - 1))) &= 0, \end{aligned} \tag{1}$$

where N is the proton density; ρ and p are the mass density and pressure in the solar wind flow, respectively; $\mathbf{V}$ is the velocity; γ is the specific heat ratio; $Q = M_i n(r)/\tau_{ion}$ is the mass loading rate by ions of mass M_i; $n(r)$ is the density of neutral atoms in the corona depending on the planetocentric distance r; and τ_{ion} is their ionization time scale.

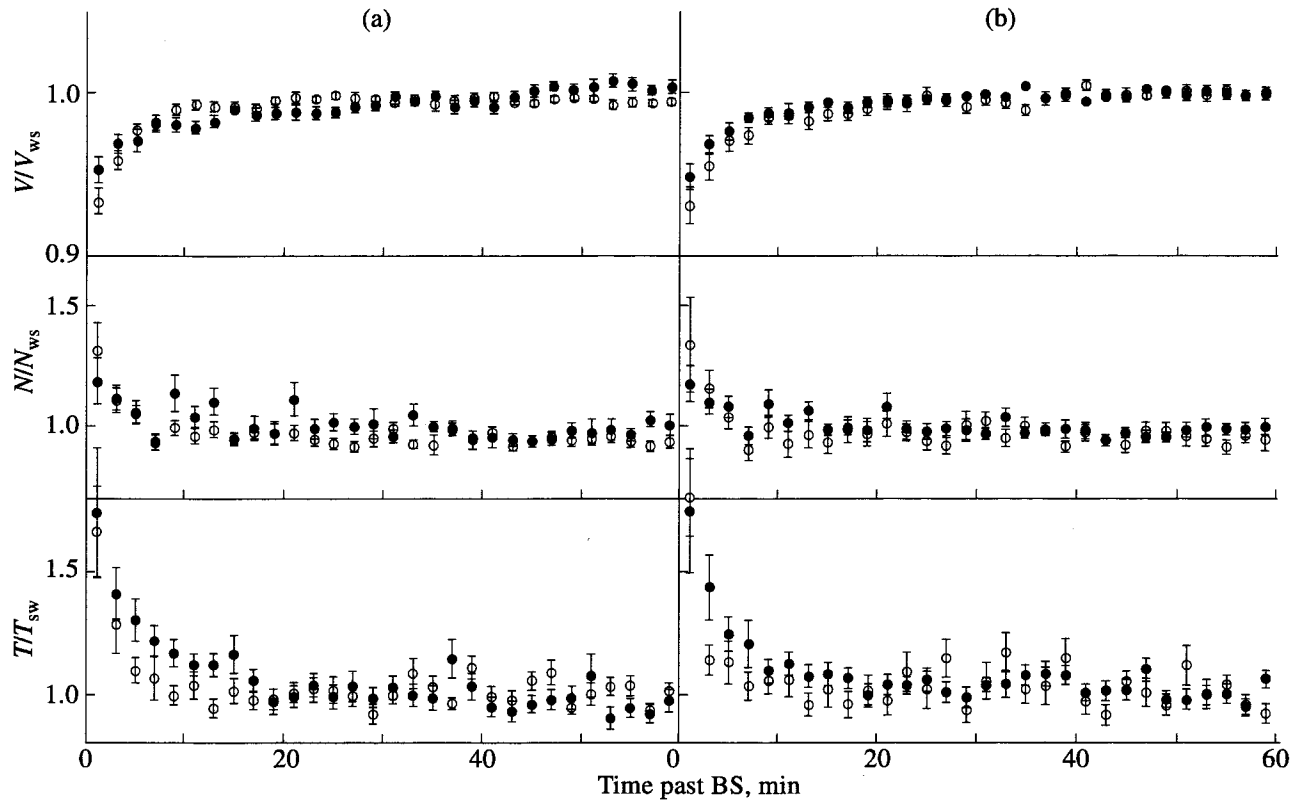

Fig. 2. Variations of average relative parameters of the solar wind upstream of the bow shock near Mars. Vertical bars mark mean-square deviations of the calculated average parameters.

In the case of the weak loading of the hypersonic flow in the linear approximation the velocity $V(r, \varphi)$ and density $N(r, \varphi)$ of solar wind protons (φ is the zenith angle, i.e., an angular distance of the point of observation and the Mars-Sun line) change along the satellite orbit according to equations [1]

$$V = V_0 - \frac{(\gamma+1)M_i n_0 r_0}{2N_0\tau_{ion}m_p}\left(\frac{r_0}{r}\right)\frac{\varphi}{\sin\varphi} \times\left[1+\frac{1}{3}\frac{n_1}{n_0}\left(\frac{r_0}{r}\right)^3\frac{\cos^3\varphi-3\cos\varphi+2}{\varphi\sin^3\varphi}\right],$$

$$N = N_0 + \frac{(\gamma-1)M_i n_0 r_0}{2V_0\tau_{ion}m_p}\left(\frac{r_0}{r}\right)\left[\left(\frac{2\varphi}{(\gamma-1)\sin\varphi} + \frac{\varphi-\sin\varphi\cos\varphi}{2\sin^3\varphi}\right)+\frac{n_1}{n_0}\left(\frac{r_0}{r}\right)^3 \times\left(\frac{2(\cos^3\varphi-3\cos\varphi+2)}{3(\gamma-1)\sin^4\varphi}+\frac{4(1-\cos\varphi)^3}{3\sin^6\varphi}\right)\right], \quad (2)$$

where V_0 and N_0 are the velocity and density of the undisturbed solar wind; m_p is the proton mass; and r_0, n_0, and n_1 are parameters of the model density profile of neutral atoms in the Martian corona [1]:

$$n(r) = n_0\left(\frac{r_0}{r}\right)^2 + n_1\left(\frac{r_0}{r}\right)^5, \quad (3)$$

where $(n_0 + n_1)$ is the density of the Martian corona at a distance $r_0 = 10^4$ km.

The equations (2) can be rewritten as follows:

$$V(r,\varphi) = V_0 - \frac{n_0 M_i r_0}{N_0\tau_{ion}} f\left(r, \varphi, \frac{n_1}{n_0}, \gamma\right),$$
$$N(r,\varphi) = N_0 + \frac{n_0 M_i r_0}{V_0\tau_{ion}} g\left(r, \varphi, \frac{n_1}{n_0}\gamma\right). \quad (4)$$

All circular orbits of the *Phobos-2* spacecraft were identical. The parameter n_1/n_0 is determined by the corona model; therefore, functions $f(r, \varphi, n_1/n_0, \gamma)$ are equal for different passes. Thus, it can be expected that the deceleration of the solar wind upstream of the bow shock $V_0 - V_s$ (V_s is the solar wind velocity just in front of the bow shock) is inversely proportional to the density of the undisturbed solar wind which determines the influence of the Martian neutral corona.

Figure 3 shows the solar wind deceleration upstream of the Martian bow shock versus the solar

wind density N_{sw} for inbound and outbound passes of the planet magnetosphere, as well as for cases where the B_m/B_{sw} ratio is greater or less than 2.3. It can be seen that for outbound passes of the magnetosphere and cases of a small jump of the magnetic field on the shock, the velocity drop is really inversely proportional to the solar wind density. However, this dependence is weak for inbound passes of the magnetosphere and for a large jump in the magnetic field. This is apparently evidence of the crucial influence of the hot oxygen and hydrogen corona on the solar wind deceleration upstream of the quasi-parallel near the planet shock wave, whereas the effect of the Martian corona is not well pronounced for quasi-perpendicular shock wave crossings because of a considerable effect of reflected protons.

For quantitative estimates it is necessary to use more exact relations accounting for different coordinates of crossing points of the Martian bow shock and the difference between the measured solar wind parameters V_{sw} and N_{sw} and the undisturbed solar wind parameters V_0 and N_0:

$$V_s = V_0 - \frac{n_0 M_i r_0}{N_0 \tau_{ion}} f_s,$$

$$V_{sw} = V_0 - \frac{n_0 M_i r_0}{N_0 \tau_{ion}} f_{sw}, \qquad (5)$$

$$N_{sw} = N_0 + \frac{n_0 M_i r_0}{V_0 \tau_{ion}} g_{sw},$$

where $f_s = f(r_s, \varphi_s, n_1/n_0, \gamma)$, $f_{sw} = f(r_{sw}, \varphi_{sw}, n_1/n_0, \gamma)$, $g_{sw} = f(r_{sw}, \varphi_{sw}, n_1/n_0, \gamma)$, the s index corresponds to a point just in front of the bow shock and the sw index corresponds to a point of the spacecraft trajectory inside the solar wind distant at ~50 min from the bow shock. It is possible to get a reduced drop in the solar wind velocity from equations (5) using a linear approximation:

$$\delta v \equiv \frac{V_{sw} - V_s}{f_s - f_{sw}} \frac{\tau_{ion}}{M_i r_0} \left(1 - \frac{V_{sw} - V_s}{f_s - f_{sw}} \frac{g_{sw}}{V_{sw}}\right) = \frac{n_0}{N_{sw}}. \qquad (6)$$

One can see from (6) that the δv value should be inversely proportional to the solar wind density.

Figure 4 shows the reduced drop of the solar wind velocity ($n_1/n_0 = 1/3$) versus the density for the same four groups of spacecraft crossings of the Martian magnetopause as presented in Fig. 3. The correlation is much better in Fig. 4 than in Fig. 3, especially for the case of shock wave crossings with a small magnetic field jump $B_m/B_{sw} < 2.3$.

One can estimate the density of neutral particles n_0 in the corona using the least-squares method, provided that the deceleration of the solar wind upstream of the bow shock near Mars is only caused by the extended corona of neutral particles in the case of a spacecraft exiting the magnetosphere or of a small jump in the magnetic field at the bow shock. That is, $n_0 = 500 \pm 10$ cm^3 and $n_0 = 590 \pm 10$ cm^3, respectively.

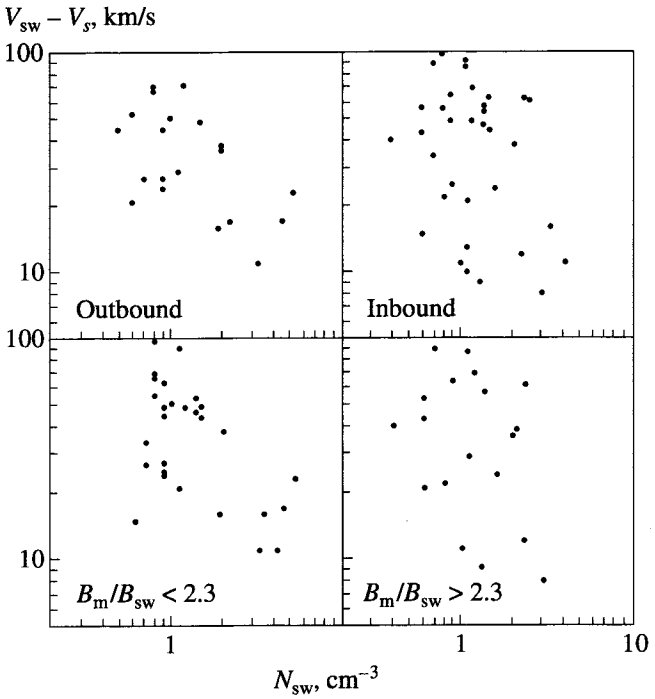

Fig. 3. The drop of solar wind velocity $V_{sw} - V_s$ versus the solar wind density N_{sw} for four groups of crossings of near Mars bow shock.

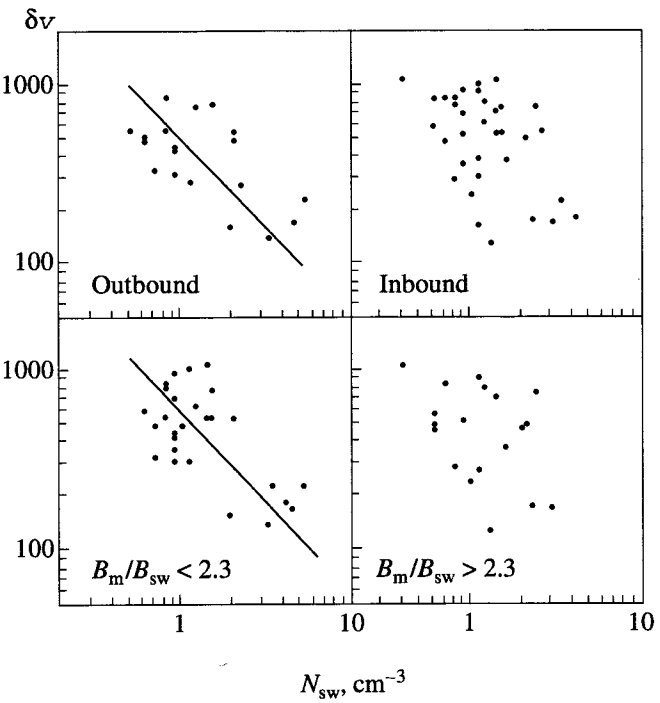

Fig. 4. Reduced drop of the solar wind velocity δv versus the density N_{sw} for the same four groups of crossings as in Fig. 3. Solid lines correspond to the data approximation with a least-squares method: $\delta v = 500/N_{sw}$ for the outbound bow shock crossings, $\delta v = 590/N_{sw}$ for bow shock crossings with a magnetic field jump $B_m/B_{sw} < 2.3$.

DISCUSSION

Measurements by the TAUS energy spectrometer aboard the *Phobos-2* spacecraft revealed a regular deceleration of the solar wind flow upstream of the Martian bow shock. The deceleration has been observed during three passes of the bow shock in the subsolar region, the data from which are available, and during a majority of passes in the terminator plane. The relative velocity drop is greater by a factor of 1.5–2 and sharper upstream of the bow shock on the dusk side than on the dawn side, where the velocity drops more gradually (Figs. 1 and 2). This difference is apparently a consequence of the fact that a quasi-perpendicular shock wave is usually observed on the dusk side, but a quasi-parallel shock wave on the dawn side.

As has been already stressed in the introduction, there are two possible causes of the deceleration of the solar wind upstream of the bow shock near Mars: the mass loading of the solar wind flow by ions originating from the neutral corona of the planet and/or by protons reflected from the bow shock.

Our analysis of the solar wind deceleration upstream of the bow shock near Mars has shown that the velocity drop is inversely proportional to the solar wind density for inbound crossings of the bow shock by the spacecraft and for bow shock crossings with a small jump on the magnetic field. This suggests that the oxygen and/or hydrogen corona near Mars governs solar wind deceleration in these cases.

The number of protons reflected from the bow shock, which may also cause the deceleration of the solar wind, depends on different solar wind parameters: the angle θ_{BN}, Mach number, plasma parameter β, specific heat ratio and others [7]. Among these parameters, only the Alfvenic Mach number M_A and β depend on the solar wind density. The fraction of reflected ions with respect to the number of incident solar wind ions apparently increases with M_A and β [7]. Therefore, the solar wind deceleration should correlate with the solar wind density in the case of determining the influence of specularly scattered protons contrary to the case of the loading of the flow by ions of planetary origin.

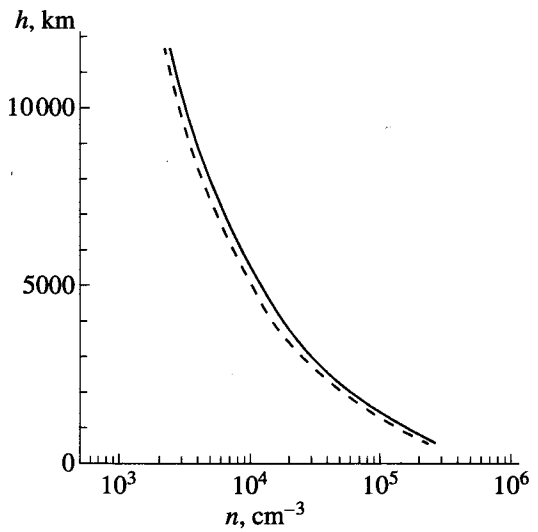

Fig. 5. Profiles of the hot oxygen density in the Martian corona. Solid line is the profile calculated in this work on the basis of the analysis of bow shock crossings near the terminator plane. Dashed line is the profile calculated in [1] using the analysis of bow shock crossings near the subsolar point.

Similarly, it is impossible to describe the obtained results by "diffusive" ions flowing from the bow shock in the foreshock region upstream of the quasi-parallel shock wave. Actually, the solar wind deceleration of 20–30 km/s upstream of the Martian bow shock (Fig. 3, left) is greater on average than the solar wind deceleration observed in the foreshock near the Earth (7–10 km/s). A value of 25–40 km/s was observed only in some individual cases [13]. The density of diffusive ions flowing from the shock waves proportional to the density of incident solar wind flow [23] and, therefore, the loading of the flow by these ions, will lead to a drop in the solar wind velocity independent of the density of the incoming flow. This contradicts the relationship considered above between the solar wind deceleration and its density for a quasi-parallel shock wave.

Assuming that the solar wind deceleration upstream of the quasi-parallel shock wave is mainly caused by the loading of the flow by ions originating from the hot oxygen corona near Mars, and applying the model of oxygen corona presented in [2, 3], one can estimate from equation (6) the parameter n_0 of the density profile of the oxygen corona given by (3): $n_0 \sim 500$–590 cm^{-3}. Figure 5 shows the density height profile (solid line) of the hot oxygen in the Martian corona. This profile is naturally more reliable near the orbit of *Phobos-2*, i.e., at a height of ~6000 km. The dashed line in this figure corresponds to the oxygen profile obtained in [1] analyzing data from the elliptical orbits ($n_0 \sim 500$ cm^{-3}, $n_1/n_0 = 1/3$). This profile is more reliable at a height of ~1500 km, where the bow shock is observed near the subsolar point. The good agreement between these profiles is clear. Therefore, the profile with parameters of $n_0 \sim 500$ cm^{-3}, $n_1/n_0 = 1/3$ describes well the solar wind deceleration upstream of the Martian bow shock in the subsolar region and agrees with the discovered correlation of the solar wind deceleration and its density in front of the quasi-parallel shock wave near the terminator plane. However, the hot oxygen density according to this profile is about 5 times higher than density values from the Ip model [2, 3], and the divergence from other models is still higher [24–26].

Generally speaking, the profile discussed above describes not only the oxygen corona of the planet, but incorporates the hydrogen corona as well. The value of the velocity drop in front of the bow shock

caused by the loading of the solar wind by ions of planetary origin is proportional to the mass of loading flow ions and the corona density, and is inversely proportional to the ionization time scale of neutral atoms of the corona (2), (4). If the hydrogen density profile $n_H(r)$ in the corona is similar to expression (3), then the obtained profile $n(r)$ is

$$n(r) = n_O(r) + n_H(r)\frac{M_H\tau_O}{M_O\tau_H} \approx 500\left(\frac{r_0}{r}\right)^2\left(1+\frac{1}{3}\left(\frac{r_0}{r}\right)^3\right), \quad (7)$$

where M_O, τ_O and M_H, τ_H are the masses and ionization time scales of oxygen and hydrogen respectively.

Picked-up protons originating from the Martian hydrogen corona were observed in the solar wind upstream of the bow shock during the ASPERA experiment on board *Phobos-2* [27]. The density of hot oxygen was never measured in the vicinity of Mars, and the density of hot hydrogen was estimated using Lyman-alpha line data obtained during the period close to the solar activity minimum aboard the *Mariner-6, 7, 9* and *Mars-2, 3* spacecraft [28, 29]. The thermal hydrogen density may be 10 times greater than the hot oxygen density during a period of solar activity minimum [24–26]. It can be assumed that the same relation would be valid for the period of *Phobos-2* observations close to the solar activity maximum.

The total ionization time scale can be estimated by an expression

$$\frac{1}{\tau_{ion}} = \frac{1}{\tau_{phot}} + \frac{1}{\tau_{ce}} + \frac{1}{\tau_{im}},$$

where τ_{phot} is the photoionization time scale, τ_{ce} is the charge exchange time scale, and τ_{im} is the time scale of electron impact. Near the orbit of Mars, the ionization time for atomic oxygen is $\tau_O \approx 2 \times 10^6$ s ($\tau_{phot} \sim 1.4 \times 10^6$ s, $\tau_{ce} \sim 4 \times 10^6$ s, $\tau_{im} \sim 2 \times 10^7$ s at a distance of 1 AU from the Sun). The ionization time for atomic hydrogen is $\tau_H \sim 3 \times 10^6$ s ($\tau_{phot} \sim 10^7$, $\tau_{ce} \sim 1.7 \times 10^6$ s, $\tau_{im} \sim 5 \times 10^7$ s at 1 AU from the Sun) [30]. Taking into account the mass difference of oxygen and hydrogen, it follows from (7) that the contribution of the hydrogen corona of Mars in the solar wind deceleration process may reach 30% of the oxygen corona contribution. Nevertheless, even accounting for the possible effect of the hydrogen corona, the oxygen density determined by the solar wind deceleration is ~3.5 times higher than the density estimated using the most extreme model [2, 3].

Barabash and Norberg state in [31] that the helium corona of Mars may also affect the mass loading of the solar wind near Mars. However, the hydrogen density exceeds the helium density beginning from a height of ~1200 km, even according to the extreme work model of Moroz [32], with exponent extrapolation to heights greater 450 km. All crossings of the Martian bow shock occurred at large heights (~1500 km near the subsolar point and ~6000 km near the terminator plane). The ionization time scale of helium is about one order of magnitude greater than the hydrogen ionization time. Therefore, the influence of the helium corona may be neglected for the solar wind deceleration upstream of the bow shock near Mars.

CONCLUSION

Plasma and magnetic field data obtained by the *Phobos-2* spacecraft in the vicinity of the Martian bow shock near the terminator plane have been analyzed.

Solar wind velocity upstream the bow shock decreases by about 7% for entry of the spacecraft into the Martian magnetosphere (dusk side) and by about ~4% for exit from the magnetosphere (dawn side), with a sharper drop of the velocity being observed on the dusk side. Observations corresponding to shock wave crossings with a large and small jump of the magnetic field differ in similar ways. This suggests that the spacecraft more often crosses a quasi-perpendicular shock wave on the dusk side, but a quasi-parallel shock wave on the dawn side.

The velocity drop is inversely proportional to the solar wind density for outbound crossings of the bow shock (quasi-parallel shock wave) by the spacecraft, but this dependence is weak for inbound crossings of the bow shock. This difference allows one to separate possible causes of the solar wind deceleration upstream of the bow shock. The mass loading of the solar wind by ions originating from the neutral corona of Mars describes well the solar wind deceleration upstream of the quasi-parallel shock wave. In the case of the quasi-perpendicular shock wave, the solar wind deceleration is caused also by protons reflected from the bow shock.

The obtained dependence of the reduced drop of solar wind velocity upstream of the bow shock for spacecraft exiting from the magnetosphere allows one to calculate a density profile of the oxygen–hydrogen corona of Mars, which is naturally more reliable at a height of ~6000 km. This height corresponds to shock wave crossings near the terminator plane. This profile agrees well with the profile calculated earlier using the data of shock wave crossings near the subsolar point [1]. However, the oxygen density determined by this profile is ~3.5 times higher than the density estimated using the extreme model [2, 3].

ACKNOWLEDGMENTS

This work was supported in part by the Russian Foundation for Basic Research (grant no. 95-02-04223), the International Science Foundation (grant no. MQU000/MQU300), the INTAS (grant no. 94-982), the Hungarian Science Foundation OTKA (grant no. T015866) and the Hungarian-Russian Interstate Program for S&T Cooperation (project no. 28).

REFERENCES

1. Verigin, M.I., Gringauz, K.I., Kotova, G.A, *et al.*, On the Problem of the Martian Atmosphere Dissipation: Phobos 2 TAUS Spectrometer Results, *J. Geophys. Res.*, 1991, vol. 96, p. 19315.
2. Ip, W.H., On a Hot Oxygen Corona of Mars, *Icarus*, 1988, vol. 76, p. 135.
3. Ip, W.H., The Fast Atomic Corona Extension of Mars, *Geophys. Res. Letters*, 1990, vol. 17, p. 2289.
4. Barabash, S. and Lundin, R., Reflected Ions near Mars: Phobos-2 Observations, *Geophys. Res. Letters*, 1993, vol. 20, p. 787.
5. Dubinin, E., Obod, D., Pedersen, A., and Grard, R., Mass-Loading Asymmetry in the Upstream Region near Mars, *Geophys. Res. Letters*, 1994, vol. 21, p. 2769.
6. Goodrich, C.C., Numerical Simulations of Quasi-Perpendicular Collisionless Shocks, in *Collisionless Shocks in the Heliosphere: Reviews of Current Research*, Geophys. Monogr. Ser., vol. 35, Tsurutani B.T. and Stone R.G., Eds., Washington, DC: AGU, 1985, p. 153.
7. Wilkinson, W.P. and Schwartz, S.J., Parametric Dependence of the Density of Specularly Reflected Ions at Quasi-Perpendicular Collisionless Shocks, *Planet. Space Sci.*, 1990, vol. 38, p. 419.
8. Onsager, T.G. and Thomsen, M.F., The Earth's Foreshock, Bow Shock, and Magnetosheath, *Rev. Geophys.*, Supplement, US National Report to International Union of Geodesy and Geophysics, 1991, p. 998.
9. Sckopke, N., Paschmann, G., Bame, S.J., *et al.*, Evolution of Ion Distributions across the Nearly Perpendicular Bow Shock: Specularly and Non-Specularly Reflected-Gyrating Ions, *J. Geophys. Res.*, 1983, vol. 88, p. 6121.
10. Gosling, J.T. and Robson, A.E., Ion Reflection, Gyration and Dissipation at Supercritical Shocks, in *Collisionless Shocks in the Heliosphere: Reviews of Current Research*, Geophys. Monogr. Ser., vol. 35, Tsurutani B.T. and Stone R.G., Eds., Washington, DC: AGU, 1985, p. 141.
11. Neugebauer, M., Initial Deceleration of Solar Wind Positive Ions in the Earth's Bow Shock, *J. Geophys. Res.*, 1970, vol. 75, p. 717.
12. Gosling, J.T., Thomsen, M.F., Bame, S.J., *et al.*, Evidence for Specularly Reflected Ions Upstream from the Quasi-Parallel Bow Shock, *Geophys. Res. Lett.*, 1982, vol. 9, p. 1333.
13. Bame, S.J., Asbridge, J.R., Feldman, W.C., *et al.*, Deceleration of the Solar Wind Upstream from the Earth's Bow Shock and the Origin of Diffuse Upstream Ions, *J. Geophys. Res.*, 1980, vol. 85, p. 2981.
14. Bonifazi, C., Moreno, G., Lazarus, A.J., and Sullivan, J.D., Deceleration of the Solar Wind in the Earth's Foreshock Region: ISEE 2 and IMP 8 Observations, *J. Geophys. Res.*, 1980, vol. 85, p. 6031.
15. Rosenbauer, H., Shutte, N., Apathy, I., *et al.*, Study of Three Dimensional Distribution Functions of Main Solar Wind Ions: Protons and Alpha-Particles in the Project "Phobos". The TAUS Experiment (Complex MPK), in *Apparatura i metody issledovaniya kosmicheskogo prostranstva* (Instruments and Methods for Space Research), Moscow: Nauka, 1989, p. 30.
16. Aydogar, O., Schwingenschuh, K., Schelch, G., *et al.*, The Phobos Fluxgate Magnetometer (MAGMA) Instrument Description, *IWF-8904*, Austrian Acad. Sci., 1989.
17. Rosenbauer, H., Shutte, N., Apathy, I., *et al.*, Ions of Martian Origin and Plasma Sheet in the Martian Magnetosphere: Initial Results of the TAUS Experiment, *Nature*, 1989, vol. 341, no. 6243, p. 612.
18. Rosenbauer, H., Shutte, N., Apathy, I., *et al.*, First Results of Measurements of Martian Origin Ions and Discovery of Plasma Layer in the Martian Magnetosphere according to Data of the TAUS Experiment aboard the Phobos-2 Spacecraft, *Pisma Astron. Zh.*, 1990, vol. 16, no. 4, p. 368.
19. Slavin, J.A., Schwingenschuh, K., Riedler, W., and Yeroshenko, Ye., The Solar Wind Interaction with Mars: Mariner 4, Mars 2, Mars 3, Mars 5 and Phobos 2 Observations of Bow Shock Position and Shape, *J. Geophys. Res.*, 1991, vol. 96, p. 11235.
20. Zhang, T.L., Schwingenschuh, K., Lichtenegger, H., *et al.*, Interplanetary Magnetic Field Control of the Mars Bow Shock: Evidence for Venuslike Interaction, *J. Geophys. Res.*, 1991, vol. 96, p. 11265.
21. Tatrallyay, M., Russell, C.T., Luhmann, J.G., *et al.*, On the Proper Mach Number and Ratio of Specific Heats for Modelling the Venus Bow Shock, *J. Geophys. Res.*, 1984, vol. 89, p. 7381.
22. Biermann, L., Brosowsky, B., Schmidt, H., The Interaction of the Solar Wind with a Comet, *Solar Physics*, 1967, vol. 1, p. 254.
23. Tratner, K.J., Möbius, E., Scholer, M., *et al.*, Statistical Analysis of Diffuse Ion Events Upstream of the Earth's Bow Shock, *J. Geophys. Res.*, 1994, vol. 99, p. 13389.
24. Nagy, A.F. and Cravens, T.E., Hot Oxygen Atoms in the Upper Atmosphere of Venus and Mars, *Geophys. Res. Lett.*, 1988, vol. 8, p. 251.
25. Nagy, A.F. and Cravens, T.E., Hot Hydrogen and Oxygen Atoms in the Upper Atmosphere of Venus and Mars, *Ann. Geophys.*, 1990, vol. 8, p. 251.
26. Lammer, H. and Bauer, S.J., Nonthermal Atmospheric Escape from Mars and Titan, *J. Geophys. Res.*, 1991, vol. 96, p. 1819.
27. Barabash, S., Dubinin, E., Pissarenko, N., *et al.*, Picked-Up Protons near Mars: Phobos Observations, *Geophys. Res. Lett.*, 1991, vol. 18, p. 1805.
28. Anderson, D.E., Mariner 6, 7 and 9 Ultraviolet Spectrometer Experiment: Analysis of Hydrogen Lyman-Alpha Data, *J. Geophys. Res.*, 1974, vol. 79, p. 1513.
29. Dostovalov, S.B. and Chuvakhin, S.D., On Distribution of Neutral Hydrogen in the Upper Atmosphere of Mars, *Kosm. Issled.*, 1973, vol. 11, no. 5, p. 767.
30. Cravens, T.E., Kozyra, J.U., Nagy, A.F., *et al.*, Electron Impact Ionization in the Vicinity of Comets, *J. Geophys. Res.*, 1987, vol. 92, p. 7341.
31. Barabash, S. and Norberg, O., Indirect Detection of the Martian Helium Corona, *Geophys. Res. Lett.*, 1994, vol. 21, p. 1547.
32. Moroz, V.I., Kerzhanovich, V.V., and Krasnopol'skii, V.A., Work Model of the Mars Atmosphere for the Mars-94 (MA-90) Project, *Kosm. Issled.*, 1991, vol. 29, no. 1, p. 3.